

Preparation of a Nonstoichiometric Sillenite-Type Phase in the System $\text{Bi}_2\text{O}_3\text{-As}_2\text{O}_5$

A. WATANABE* AND S. TAKENOUCI

National Institute for Research in Inorganic Materials, 1-1 Namiki, Tsukuba-shi, Ibaraki, 305 Japan

AND P. CONFLANT, J.-P. WIGNACOURT, M. DRACHE,
AND J.-C. BOIVIN

Laboratoire de Cristallographie et Physicochimie du Solide, URA CNRS 452, ENSCL et USTLFA, B. P. 108, 59652 Villeneuve d'Ascq Cedex, France

Received April 14, 1992; in revised form July 30, 1992; accepted August 3, 1992

This paper describes a nonstoichiometric sillenite-type phase found in the bismuth-rich portion of the system $\text{Bi}_2\text{O}_3\text{-As}_2\text{O}_5$. This phase, with body-centered cubic (BCC) symmetry, forms a solid solution over an extremely limited range between 6.23 and 6.74 ± 0.01 mol% As_2O_5 at 650°C. A sample with the composition of 6.52 mol% As_2O_5 shows two phase transitions at 816°C and 889°C, respectively, and melts incongruently at 941°C. In the heating direction the 816°C transition is due to a structural change from the BCC to a monoclinic superstructure based on hexagonal LaOF-type subcells; the monoclinic phase might be expected to be an oxide-ion conductor. A structural model for the nonstoichiometric sillenite-type phase is discussed from the point of view that all the tetrahedral sites are statistically filled by Bi^{3+} and As^{5+} ions. © 1993 Academic Press, Inc.

Introduction

A body-centered cubic (BCC) phase with space group $I23$ and a ≈ 10 Å frequently occurs in the bismuth-rich region in the many systems of bismuth mixed oxides and is referred to as a sillenite-type (S-type) phase. Usually this phase has the stoichiometric composition $\text{Bi}_{12}\text{MO}_{20}$, where M denotes a cation of the additive oxide or a suitable combination of cations of oxides. The crystal structure was determined by Abrahams *et al.* (1) for $\text{Bi}_{12}\text{GeO}_{20}$; the result

showed that the tetrahedral sites corresponding to the special positions $2a$ in $I23$ are occupied by two M cations and two formula weights are contained in the unit cell.

Nonstoichiometric S-type phases have also been reported by several workers (2-9). To date, little is known about relationships between the nonstoichiometric composition and the atomic position. However, on the basis of the assumption of the presence of Bi^{5+} , Watanabe *et al.* (7) proposed a cation-deficient model for the nonstoichiometric S-type phase with 6.73 mol% P_2O_5 found in the system $\text{Bi}_2\text{O}_3\text{-P}_2\text{O}_5$; that is, $\text{Bi(III)}_{23.33}[\text{Bi(V)}_{0.295}\text{P}_{1.705}]_{40}\text{O}_{40}$. This

* To whom correspondence should be addressed.

means that the Bi^{3+} ions are always vacant by only 2.78% in the S-type phase of the system $\text{Bi}_2\text{O}_3\text{-Bi}_2\text{O}_5\text{-M}_2\text{O}_5$. Thus, this structural model induced us to study the phase equilibria in the bismuth-rich region of the system $\text{Bi}_2\text{O}_3\text{-As}_2\text{O}_5$ with a view to confirming the existence of the nonstoichiometric S-type phase.

Experimental Procedure and Results

The starting materials were 99.9% pure Bi_2O_3 (Iwaki Chemicals, Ltd.) and 99.999% pure As_2O_5 (Soekawa Chemicals, Ltd.). Polycrystalline specimens of composition $\text{Bi}_{2-2x}\text{As}_{2x}\text{O}_{3+2x}$ (where $x = 0.02$ to 0.15) were prepared by solid-state reactions. The desired proportions were accurately weighed and homogenized well in an agate mortar. A mixture was transferred into a covered gold crucible and heated at 650°C for 40 hr. Samples were then quenched by an airstream to room temperature. All samples were checked by X-ray powder diffraction (XRPD) with Ni-filtered $\text{CuK}\alpha$ radiation. When the reaction was incomplete after a single heat treatment, the mixture underwent another similar heat treatment. The XRPD patterns suggested that the S-type phase has a very narrow solid-solution region around 6.5 mol% As_2O_5 .

Since the starting material for As_2O_5 was deliquescent and since the correct composition of the final product is essential for a close examination into the nonstoichiometry, chemical analyses were conducted using a colorimetric method by the molybdenum blue reaction (10) for the determination of arsenic content and using a chelatometric titration with EDTA (xylenol orange indicator and $\text{pH} < 1$) (11) for that of bismuth content. The final content of each element is obtained by averaging the four measured values for bismuth and by averaging the two measured ones for arsenic. As a result, for example, a sample with nominal composition of 93.5 mol% $\text{Bi}_2\text{O}_3/6.5$ mol% As_2O_5

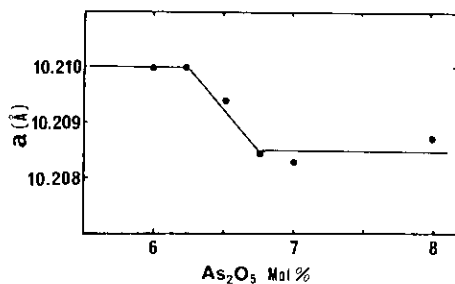


FIG. 1. Variation of lattice constant of the sillenite-type solid solution at 650°C with As_2O_5 content in the system $\text{Bi}_2\text{O}_3\text{-As}_2\text{O}_5$.

turned out to contain 93.47 mol% $\text{Bi}_2\text{O}_3/6.53$ mol% As_2O_5 actually. The probable error was estimated to be ± 0.01 mol%.

The precise lattice constant was determined by applying the least-squares treatment to 16 independent reflections selected in the $2\theta = 58^\circ\text{-}122^\circ$ region with $\text{CuK}\alpha$ radiation and a diffracted-beam monochromator. The results of the S-type single phase are as follows: $a = 10.2101(1)$ Å for a composition with 6.23 mol% As_2O_5 , $a = 10.2097(1)$ Å with 6.53 mol% As_2O_5 , and $a = 10.2094(0)$ Å with 6.52 mol% As_2O_5 .

To obtain solid solubility limits of the S-type phase by the parametric method (12), the lattice parameter was plotted against actual As_2O_5 content as shown in Fig. 1. It turned out that the S-type solid solution was formed over a limited compositional range, between 6.23 and 6.74 ± 0.01 mol% As_2O_5 at 650°C . The linear relationship indicates that the homogeneity of the sample is sufficient.

The differential thermal analysis (DTA) was carried out as described previously (13). Figure 2 represents a DTA curve for a specimen with 6.52 mol% As_2O_5 . In the heating direction three endothermic peaks are observed, one at 816, one at 889, and one at 941°C ; however, in the subsequent cooling curve all exothermic peaks do not correspond to those of the heating process. This result suggests that phase relations

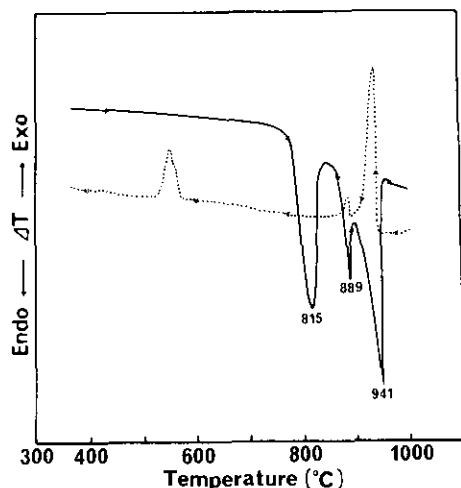


FIG. 2. DTA curve for a sample with composition 6.52 mol% As_2O_5 measured at a rate of $10^\circ\text{C min}^{-1}$. The solid line is a heating curve and the dotted line a cooling one.

around the present solid solution are fairly complex.

To check structural changes at the two endothermic effects of 816°C and 889°C below the melting point of 941°C , a high-temperature XRPD (HTXRPD) method was used on the sample with the same composition 6.52 mol% As_2O_5 . A diffraction pattern was continuously recorded by a Guinier-Lenne camera under conditions of sample heating to a maximum temperature of 925°C at a rate of about 18°C hr^{-1} . A clear result is shown in Fig. 3: at about $802 \pm 4^\circ\text{C}$ the BCC phase starts to transform into a high-temperature phase; in other words, another phase appears suddenly around this temperature. The 816°C endothermic peak in the DTA heating curve is ascribed to this structural change. The transformation temperature by HTXRPD is somewhat lower than that by DTA, because the dimensional change may be premonitory symptom of the true transition (14). The high-temperature phase consists of hexagonal LaOF-type (15) related subcells, because many weak super-

lattice lines are recognized besides the LaOF-type fundamental lines. Measured diffraction lines, except for two lines, could be tentatively indexed on the basis of a monoclinic lattice with $a = 6.922 \text{ \AA}$, $b = 9.798 \text{ \AA}$, $c = 6.888 \text{ \AA}$, and $\beta = 120.2^\circ$. The results are listed in Table I; the unindexed weak lines suggest that the true cell may be larger than the tentative one. On the other hand, no explicit structural change is observed around the second endothermic peak temperature of 889°C . This means that the transition may be a displacive one which can be related to the far smaller DTA peak, i.e., the heat of transition.

The dc conductivity measurement was performed in the same way as reported elsewhere (16). Figure 4 shows the plot of $\log(\sigma) - 1/T$ for the specimen with composition 6.52 mol% As_2O_5 . The result indicates that a reversible change occurs around 800°C with a remarkable hysteresis. In accordance with the results of both high-temperature XRPD and DTA, this change corresponds to the polymorphic transition between the S-type phase and the monoclinic high-temperature phase.

Discussion

The present S-type phase appeared around similar composition to that in the system $\text{Bi}_2\text{O}_3\text{-P}_2\text{O}_5$, in which the phase is what is called a line compound with 6.73

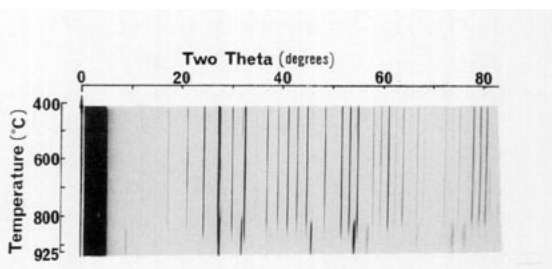


FIG. 3. High-temperature XRPD pattern of a sample with 6.52 mol% As_2O_5 using $\text{Cu K}\alpha$ radiation; the sample was heated continuously at a rate of about 18°C hr^{-1} and kept at a maximum temperature of 925°C .

TABLE I
X-RAY POWDER DIFFRACTION DATA FOR
93.48 Bi₂O₃ · 6.52 As₂O₅ AT 875°C

<i>h</i>	<i>k</i>	<i>l</i>	<i>d</i> _{calc} (Å)	<i>d</i> _{obs} (Å)	<i>I</i> _{obs}
0	1	0	9.798	9.764	W
	—		—	8.418	VW
	—		—	5.941	W
0	1	1	5.087	5.085	W
0	2	1	3.782	3.779	VW
1	0	1	3.440	3.441	VW
0	3	0	3.266	3.270	MS
1	1	1	3.246	3.248	VS
0	3	1	2.863	2.864	VW
0	1	2	2.847	2.853	VW
1	2	-2	2.818	2.818	VS
0	2	2	2.543	2.542	VW
1	3	1	2.369	2.363	VW
1	0	-3	2.252	2.252	VW
2	1	1	2.198	2.197	VW
2	2	1	2.049	2.047	VW
1	4	1	1.996	1.997	MS
0	0	3	1.984	1.988	MS
1	5	-2	1.703	1.706	S
0	3	3	1.696	1.698	S
2	1	-4	1.696	1.696	S
0	6	0	1.633	1.635	M
2	2	2	1.623	1.625	M
2	4	-4	1.409	1.409	W
1	7	1	1.297	1.296	W
2	5	2	1.293	1.291	W
1	1	4	1.288	1.287	W
0	6	3	1.261	1.260	W
1	2	-5	1.256	1.255	W

mol% P₂O₅ (7). On the other hand, Devalette *et al.* (5) and Horowitz *et al.* (9) reported a line compound with 6.25 mol% As₂O₅, and Shashchanova *et al.* (17) described a compound with 5 mol% As₂O₅. Devalette *et al.* (5) proposed a structural model, which is devoid of the tetrahedral site by 20%, Bi(III)₂₄[As(V)_{1.6}□_{0.4}]O₄₀, where □ stands for the tetrahedral site vacancy. As can be seen, this model is effective only with the composition of 6.25 mol% As₂O₅. When the As₂O₅ content is higher than 6.25 mol%, the number of O²⁻ ions is in considerable excess of that structurally required (1, 7); in contrast, the lower As₂O₅

content brings about a further deficit of both tetrahedral 2*a* sites and oxygen sublattice. As shown in the next paragraph, the negligible vacancy is contained in the oxygen sublattice of the S-type phase with P₂O₅, As₂O₅, or V₂O₅. Furthermore the present study gives not a line compound with 6.25 mol% As₂O₅ but a solid solution over 6.23–6.74 mol% As₂O₅. Thus, a chemical formula for the present S-type phase can be represented in the same manner as described previously (7) on the assumption that no vacancy is generated in the oxygen sublattice as well as in the tetrahedral 2*a* sites which are randomly occupied by both Bi⁵⁺ and As⁵⁺ ions. That is, Bi(III)_{23.33}[Bi(V)_{2-2*x*}As(V)_{2*x*}]O₄₀, where *x* = 0.79–0.85. As mentioned in the Introduction, this type of chemical formula might be given to the S-type phase which appears in the binary system of Bi₂O₃ with a pentavalent oxide such as P₂O₅, As₂O₅, or V₂O₅.

The results shown in Fig. 4 may suggest that the relatively high electrical conductivity of the S-type phase is perhaps attributed to oxide ions in whole. If this is true, we have to take the oxygen deficient model into

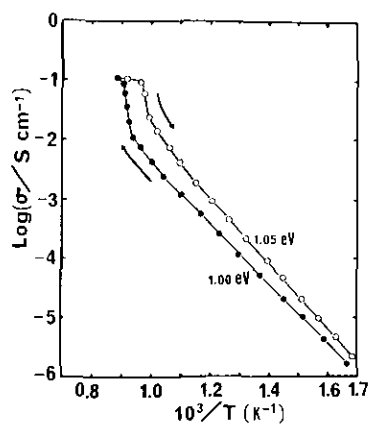


Fig. 4. Arrhenius plots of electrical conductivity σ for the first heating and cooling cycle in air of a sample with 6.52 mol% As₂O₅. Solid circles are σ 's during heating and open circles are σ 's during cooling. Activation energies are inset.

consideration. However, Wignacourt *et al.* (8) reported that the measurements of oxide-ion transport number for the S-type phase indicate less than 0.5 in the system $\text{Bi}_2\text{O}_3\text{-P}_2\text{O}_5$, in which the phase forms a solid solution over 5–7.15 mol% P_2O_5 . Furthermore, Soubeyroux *et al.* (18) elucidated no oxygen vacancy in the S-type phase with V_2O_5 using neutron diffraction, although their structural model, $\text{Bi(III)}_{24}[\text{Bi(V)}_{1.5}\text{V(V)}_{0.1}\square_{0.4}]\text{O}_{40}$ and composition are different from the present one. Thus, we can conclude from these evidences that the S-type phase with P_2O_5 , As_2O_5 , or V_2O_5 has negligible vacancy in the oxygen sublattice.

The monoclinic high-temperature phase with hexagonal LaOF-type related subcells exhibits fairly good electrical conductivity (above 838°C in Fig. 4). Since the hexagonal LaOF-type structure is closely related to the fluorite-type one (15), and since $\delta\text{-Bi}_2\text{O}_3$, which is the high-temperature modification stable between 730 and 825°C (19, 20), has an oxygen-deficient fluorite-type structure (21) and shows excellent oxide-ion conductivity (22), the present high-temperature phase might be expected to be an oxide-ion conductor. Likewise, the S-type phase in the system $\text{Bi}_2\text{O}_3\text{-P}_2\text{O}_5$ underwent a polymorphic transition (7) and a high-temperature phase turned out to have the same structure (23) as that of the present high-temperature phase; in addition, for this high-temperature phase with P_2O_5 the oxide-ion transport number was in the vicinity of unity (8). Thus, by analogy with similar systems, the present high-temperature phase with As_2O_5 would seem to be a good oxide-ion conductor.

We checked the system $\text{Bi}_2\text{O}_3\text{-As}_2\text{O}_5$ partly to make a comparison between this and the present system $\text{Bi}_2\text{O}_3\text{-As}_2\text{O}_5$. The starting As_2O_5 powder (CERAC Inc.) was 99.999% pure, and the sample preparation was the same as described above. As a result, the S-type phase appeared in this system and formed a solid solution with a nar-

row compositional region. However, contrary to expectation, it turned out by the chemical analysis (10) that most of the As^{3+} ions are oxidized into As^{5+} in this S-type phase. Therefore the actual composition of this S-type phase in the system $\text{Bi}_2\text{O}_3\text{-As}_2\text{O}_5$ could be described by As_2O_5 content: the solid solution is formed over approximately 6.1–6.4 mol% As_2O_5 . That is, the incorporation of As^{3+} ions into Bi_2O_3 does not lead to an S-type phase such as $\text{Bi}_{24}[\text{As(V)}, \text{As(III)}]\text{O}_{40}$ or $\text{Bi}_{24}[\text{Bi(V)}, \text{As(III)}]\text{O}_{40}$ by the solid-state reaction in air.

In conclusion, the cation-deficient non-stoichiometric S-type phase was found in the system $\text{Bi}_2\text{O}_3\text{-As}_2\text{O}_5$: this phase forms a narrow solid solution region (6.23–6.74 mol% As_2O_5 at 650°C) and transforms at 816°C to a monoclinic phase which has a superstructure based on hexagonal LaOF-type subcells and which shows a good electrical conductivity probably owing to oxide ions.

Acknowledgments

One of the authors (A. Watanabe) thanks the Ecole Nationale Supérieure de Chimie de Lille and the Arai Science and Technology Foundation for their financial support.

References

1. S. C. ABRAHAMS, P. B. JAMIESON, AND J. L. BERNSTEIN, *J. Chem. Phys.* **47**, 4034 (1967).
2. E. M. LEVIN AND R. S. ROTH, *J. Res. Natl. Bur. Stand., Sect. A* **68**, 197 (1964).
3. V. N. BATOG, V. I. PAKHOMOV, G. M. SAFRONOV, AND P. M. FEDOROV, *Inorg. Mater. (Engl. Transl.)* **9**, 1400 (1973).
4. A. ROZAJ-BRVAR, M. TRONTELI, AND D. KOLAR, *J. Less-Common Met.* **68**, 7 (1979).
5. M. DEVALETTE, G. MEUNIER, J.-P. MANAUD, AND P. HAGENMULLER, *C. R. Seances Acad. Sci. Sér.* **2** **296**, 189 (1983).
6. N. KHACHANI, M. DEVALETTE, AND P. HAGENMULLER, *Z. Anorg. Chem.* **533**, 93 (1986).
7. A. WATANABE, H. KODAMA, AND S. TAKENOUCHI, *J. Solid State Chem.* **85**, 76 (1990).
8. J.-P. WIGNACOURT, M. DRACHE, P. CONFLANT, AND J.-C. BOIVIN, *J. Chim. Phys.* **88**, 1939 (1991).

9. H. S. HOROWITZ, A. J. JACOBSON, J. M. NEWSAM, J. T. LEWANDOWSKI, AND M. E. LEONOWICZ, *Solid State Ionics* **32/33**, 678 (1989).
10. E. B. SANDELL, "Colorimetric Determination of Traces of Metals," 3rd ed., p. 282, Interscience, New York (1959).
11. A. I. VOGEL, "A Text-Book of Quantitative Inorganic Analysis Including Elementary Instrumental Analysis," 3rd ed., p. 810, Longmans, London (1961).
12. B. D. CULLITY, "Elements of X-Ray Diffraction," 3rd printing, pp. 353-358, Addison-Wesley, Reading, MA (1967).
13. A. WATANABE AND H. KODAMA, *J. Solid State Chem.* **35**, 240 (1980).
14. H. D. MEGAW, "Crystal Structures: A Working Approach," p. 439, Saunders, Philadelphia (1973).
15. A. F. WELLS, "Structural Inorganic Chemistry," 4th ed., p. 405, Clarendon, Oxford (1975).
16. A. WATANABE AND T. KIKUCHI, *Solid State Ionics* **21**, 287 (1986).
17. R. B. SHASHCHANOVA, B. K. KASENOV, A. Z. BEILINA, AND V. P. MALYSHEV, *Izv. Vyssh. Uchebn. Zaved., Tsvetn. Metall.* (3) **27** (1989).
18. J. L. SOUBEYROUX, M. DEVALETTE, N. KHACHANI, AND P. HAGENMULLER, *J. Solid State Chem.* **86**, 59 (1990).
19. E. M. LEVIN AND R. S. ROTH, *J. Res. Natl. Bur. Stand. Sect. A* **68**, 189 (1964).
20. H. A. HARWIG AND A. G. GERARDS, *Thermochim. Acta* **28**, 121 (1979).
21. H. A. HARWIG, *Z. Anorg. Allg. Chem.* **444**, 151 (1978).
22. T. TAKAHASHI, H. IWAHARA, AND Y. NAGAI, *J. Appl. Electrochem.* **2**, 97 (1972).
23. P. CONFLANT, Private communication (1991).